Polycarboxylate / nanosilica modified quaternary cement formulations – enhancements and limitations

Styliani Papatzani[1,2,*] and Kevin Paine[1#]

[1]*BRE Centre for Innovative Construction Materials, University of Bath, BA2 7AY, Bath, UK*

[2] Hellenic Ministry of Culture, General Directorate of Restoration of Medieval & Post-medieval Monuments, Tzireon 8-10, 11742, Athens, Greece, Country

*Corresponding author: E-mail: spapatzani@gmail.com, Tel +30 6985877730, ORCID ID 0000-0001-8475-8975

Second author: E-mail: k.paine@bath.ac.uk ORCID ID 0000-0001-7455-7002

The effect of polycarboxylate / nanosilica (nS) particles in quaternary cement formulations comprising of Portland cement (PC), limestone powder (LS) and fly ash (FA) was investigated for the first time. The reference formulation, contained 60% PC, 20% LS and 20% FA by mass of binder in an effort to minimize clinker and maximize other constituents. nS particles were characterized via transmission and X-ray scanning electron microscopy. Nanosilica was added at a 0.3 or 0.6% by mass as a partial replacement of PC and different water-to-binder (w/b) ratios were explored. Compressive strength tests and thermal gravimetric analyses (TGA) performed at day 7, 28 and 56 testified to pozzolanic behavior. Results suggest a mechanism of "de-activation" of some FA particles with age. A new ratio; [(compressive strength in MPa)/(calcium hydroxide content detected by TGA)] was introduced, correlating

microscale characteristics (hydration products) and macroscale performance (delivered compressive strengths).

Back scattered SEM images confirmed the C–S–H network formation, the presence of reacted/unreacted FA particles, and the availability of $Ca(OH)_2$ for delayed hydration reactions. Tests on mortars also confirmed the enhancement offered by nS addition. The lower bound nS addition was determined to be 0.6% by mass of binder for pastes and 0.5% for mortars.

Keywords: Polycarboxylate nanosilica, TGA/dTG, SEM/EDX, quaternary cements

1. Introduction

Concrete structures affect the quality of our lives, while construction, rehabilitation and maintenance costs affect the economic growth of countries. In fact, the production of cement, the main constituent of concrete, comprises one of the largest industries globally. On the other hand, Portland cement (PC) clinker is responsible for about 8% of the manmade carbon dioxide emissions (Meyer 2009). The need to build ever more, is, therefore, calling for innovative cementitious binders tailored to meet specific requirements in terms of durability, performance and environmental impact. Currently, nanotechnology comprises a major stakeholder in sustainable cement production. Actually, cement nanocomposites are developed and investigated in an effort to minimize Portland cement content and maximize supplementary cementitious materials content, (usually industrial by-products such as fly ash (FA) or silica fume). Indeed, the synergistic effect of FA and LS in ternary cement formulations containing clinker, limestone and FA is confirmed offering a new way forward (De Weerdt, Kjellsen, et al. 2011). Nanoparticles can assist in the amplification of these effects. The characteristics of a material are remarkably altered when its size is reduced to the nanolevel. Therefore, the

introduction of nanoparticles in cement, will affect hydration reactions, strength and microstructure of the pastes (Singh et al. 2013).

Nanosilica (nS) particles can be suspended in water (aqueous suspensions) or other mediums. Very few studies have been published on the effect of nanoparticles in composite cementitious binders, in light of the need for CO_2 footprint reduction. Recent research by the authors' team has demonstrated the favourable effect colloidal aqueous nanosilica (nS) has on calcium silicate formation (Björnström et al. 2004) and particularly in ternary cement combinations (Portland cement 60%, limestone 40% by mass of binder and nS as PC replacement) with the enhanced consumption of $Ca(OH)_2$ towards the production of additional C–S–H, witnessed via thermal gravimetric analyses (TGA) (Papatzani 2016; Papatzani, Paine & Calabria-Holley 2014). Indeed, the addition of nS offers increased pozzolanic reactions and provides nucleation sites for additional C–S–H growth, which increase the bound water. Therefore, although the increase in C–S–H due to the amorphous nature of the hydrate is X-ray diffraction silent, it can be observed via thermal gravimetric analysis (TGA). Furthermore, the densification of the hydrated matrix, was observed with the help of scanning electron microscopy (SEM) and the increased compressive strength with strength tests for up to 170 days aged composite pastes. The optimal dosage of nS was investigated in four different mix proportions and was concluded to be 0.1% nS by total mass of binder (Папатзани et al. 2014). Further to this, quaternary combinations of colloidal aqueous nanosilica having a low PC-to-FA ratio (Portland cement 43%, limestone 30%, FA 37% by mass of binder and nS as PC replacement) exhibited significant pozzolanic behavior, investigated by TGA and compressive strength tests from day 1 until day 90, with an optimum nS content determined at 0.5% by total mass of binder (Papatzani, Paine & Calabria-Holley 2014). Fourier transform infrared spectroscopy (FTIR) investigations on quinary and quaternary pastes showed evidence of an intricate C–S–H network of honey-comb structure rather than flake-like C–S–H network of ternary pastes

(Calabria-Holley & Papatzani 2014). In addition to this, it was found that the Ca/Si ratio of the C–S–H resulting from the addition of nS particles is lower than that of the reference paste, possibly signaling denser calcium silicate hydrate gel, which in combination with the presence of FA can lead to more durable pastes (Raki et al. 2010; Calabria-Holley & Papatzani 2014).

On the other hand, polycarboxylate agents are extensively used as water reducers for concrete production. Furthermore, nS particles dispersed in a polycarboxylate medium promise water reduction capacity due to the repulsion and steric hindrance of the hydrating cement particles preventing coagulation (Shu et al. 2016) while at the same time allowing for greater strength development.

To the best knowledge of the authors, this is the first study on the effect of polycarboxylate dispersed nS on the hydration, mechanical strength and microstructure of composite cement formulations (three or more constituents). This research is focused on the binder optimization through the comparison of three different water-to-binder ratios on quaternary pastes, containing PC, FA, limestone (LS) and nS. One of the challenges of this study was to create a Portland-composite binder with high limestone content and lower than the permissible clinker content according to EN 197-1 (CEN 2000). In fact, for CEMII/A-L cements, the permissible clinker content lies within 80-95% by mass of binder and the allowable limestone content is restricted to 6-20%. As for the Portland-composite cements, i.e. cements that contain both fly ash and limestone at a total maximum of 35%, the allowable amount of clinker must not be less than 65% according to the Eurocodes. In the present study, the limestone (20%) plus fly ash content (20%) of the reference paste reached 40%, while the clinker was at 60% by total mass of solids, dissociating from current EU standards. Therefore, the ratio PC/FA/LS content was equal to 3/1/1. The effect of polycarboxylate/nS particles on the hydration reactions, microstructure and strength development was investigated together with any possible competitive reactions between FA and nS. Rheology / consistency (slump) studies or studies in

concrete formulations were beyond the scope of the present work. Mortars of binary combinations were also prepared and tested in compression (up to 90 days aged mortars) and late age relative density in order to confirm the water reducing potentials and strength enhancement offered by the addition of nS.

The research reported was part of a much broader research project supported by the EU involving industrial and academic partners throughout Europe, aiming at optimizing nanotechnology enhanced cements formulations.

2. Materials and Methods

2.1 Materials

The materials used were:

- Portland limestone cement CEMII/A-L42.5, with a limestone content of 14%, conforming to EN 197-1. The Portland cement (PC) content 86% by mass was considered separately from the limestone (LS) content (14% by mass), in order to be able to adjust the total limestone content of the composite binders. According to the supplier clinker is composed of: 70% C_3S, 4% C_2S, 9% C_3A, 12% C_4AF.
- Limestone (additional), conforming to EN 197-1. The total LS content was assigned to each paste
- Fly ash (FA), conforming to EN 450, with mean diameter of 9.09 μm. According to the supplier the oxide composition is as follows: 53.5% SiO_2, 34.3% Al_2O_3, 3,6% Fe_2O_3, 4.4% CaO.
- Commercially available colloidal amorphous polycarboxylate dispersed nS particles (GnS) 15% solids. According to the supplier the diameter of the GnS particles ranges between 3 and 150 nm and the specific surface area lies between 20 – 1000 m^2/g.

2.2 Methods

2.2.1 Experimental Procedure – Mix design

A. Quaternary cement paste formulation

PC60LS20FA20 was nanomodified with GnS at two different concentrations for three different water to binder (w/b) ratios. GnS was commercially described as "water reducing admixture with nS particles", therefore, this series of formulations were designed to assess this piece of information. Moreover, it was recommended by the supplier that the GnS addition should be between 0.5-3.0% by mass of Portland cement, hence for these pastes (containing 60%PC) the lowest permissible GnS solids content would be 0.3%. The three formulations are shown in the table below:

Table 1: GnS modified quaternary cement paste formulations - Mix proportions % by total mass of solids

Sample	**PC (%)**	**LS (%)**	**FA (%)**	**GnS (%solids)**	**W/B**
PC60LS20FA20@0.3	60.0	20.0	20.0	0.0	0.30
PC59.5LS20.1FA20.1+0.3% GnS @0.3	59.5	20.1	20.1	0.3	0.30
PC59.5LS20.1FA20.1+0.3% GnS@0.2	59.5	20.1	20.1	0.3	0.20
PC58.6LS20.4FA20.4 +0.6% GnS @0.22	58.6	20.4	20.4	0.6	0.22

The following methodology was adopted for the mixing procedure:

- Dry mixing of the powders (Portland limestone cement, fly ash and additional limestone) for 5 minutes with a spatula by hand. The quantities of materials are low, the mixing time high so adequate homogeneity is attained.
- For formulations containing GnS, the nS solution was poured in a separate container together with water, stirred with the use of a magnetic stir bar for 1 minute and then added to the mixed powders.
- With the addition of water and nS, the paste was mixed with the help of an automatic dual shaft mixer at 1150 rpm for 3 minutes for pastes up to 300 g, time increasing with amounts of paste. For 500 g mixing time was 5 minutes to ensure greater homogeneity of the pastes.

B. Mortar formulation

Three different mortars formulations were prepared in an automatic mixer complying with EN -196-Part 1 (BS 2005) mixing times. The w/b ratio of the control mix was equal to 0.5, according to the standard. Distilled water and standard sand were used. The proportions by mass according to the standard were: one part of the cement, three parts of CEN Standard sand, and one half part of water (water/binder ratio 0.50).

Apart from the control mix, two mortar specimens containing 0.5% or 0.25% GnS by mass of binder at w/b = 0.35 were also created to assess the water reducing capacity of GnS. GnS was added in the last 30 seconds of high speed mixing.

159 **C. GnS modified cement paste formulations - Casting, demoulding and curing**

160 All nanomodified pastes, were cast into cylindrical moulds of dimensions of approximately 60
161 mm height and 30 mm diameter, so as to maintain a height-to-diameter ratio value of 2 for
162 compressive strength tests. The GnS dispersion increased the fluidity of the GnS modified
163 pastes. As shown in Figure 1, these pastes were flowing when casted in the moulds. Therefore,
164 the compressive strength at day 1 was unattainable due to the fact that setting was still
165 unaccomplished by day 1 at these water to binder ratios. Rheology studies, fluidity and slump
166 were beyond the scope of this work. However, it should be noted that although the minimum
167 permissible nS content was low (0.3% of solids), for a water to binder ratio of 0.3 the paste was
168 flowing (Figure 1). Reducing the w/b ratio to 0.2, also reduced the fluidity whereas for the
169 0.6% nS addition at 0.22 w/b ratio the fluidity was similar to the w/b = 0.2 paste.

170

171 Figure 1: GnS nanomodified cement pastes

172

173 Cylindrical composite cement paste specimens were vibrated and were air cured in dry sealed
174 conditions at 20±2ºC for the first 24 hours. Consequently, after day 1, they were demoulded

and placed in a curing tank filled with distilled water at 20±2 ºC until the selected ages for compressive strength testing (day 7, 28 and 56). Separate samples of the pastes were kept in sealed, airtight bags for the first 24 hours, then filled up with water at 20±2 ºC for chemical or microstructural characterisation. Distilled water was chosen for compliance with testing standards. The use of ordinary tap water was beyond the purpose of the current work.

2.2.2. Material preparation and Analytical techniques

A. GnS characterization

At first the GnS solution was characterized in terms of shape and size via Transmission Electron Microscopy and elemental composition via scanning electron microscopy/ X-ray energy dispersive spectroscopy (SEM/EDX). GnS suspension has also been investigated via Fourier transform infrared spectrometry elsewhere (Calabria-Holley et al. 2015).

Transmission Electron Microscopy (TEM)

Suspensions at 10ng/ml were prepared from the GnS with distilled water. Small drops of the diluted solutions were then deposited on copper mesh grids coated with a thin carbon film. Grids were dried at 25°C prior to the insertion in the instrument. Samples were examined at a voltage of 120 kV with a GATAN Jeol JEM 1200 mkII. Images were recorded on a Gatan Dual View camera.

Scanning electron microscopy/ X-ray energy dispersive spectroscopy (SEM/EDX)

For SEM/EDX elemental composition analyses the GnS dispersion was first vacuum dried for three days at a pressure of 10-2 mbar (100 Pa). The dried dispersion samples were placed uncoated on a sheet of molybdenum, an element absent from the GnS dispersions for unbiased

197 elemental analyses. A matrix of 5 x 5 spectra was acquired and the median of the elemental
198 composition was presented. Samples were imaged using a Jeol 6480 LV SEM.

199

200 B. GnS enhanced cement pastes characterization

201 For the paste characterization, arrest of hydration was performed following two different
202 methodologies: solvent exchange and oven drying as described by Calabria-Holley et al.
203 (2014). For SEM back scattered images generation and microstructural investigation, solvent
204 exchange was the technique employed for the arrest of hydration. Isopropanol was selected as
205 the most appropriate solvent according to literature (Zhang & Scherer 2011; Bye et al. 2011).
206 The thermal properties were investigated via thermal gravimetric analysis and differential
207 thermogravimetry (TGA/dTG). For TGA/dTG, the oven drying technique was adopted.

208

209 **Compressive strength tests -** Compressive strength tests of mortars were carried out in
210 accordance with EN 196-1. For the compressive strength tests of cement pastes, tests were
211 carried out on up to six cylindrical specimens per mix. All samples were tested at a loading
212 speed of 0.5MPa/s. The value of strength was obtained from the mean of the specimens tested
213 and therefore, the compressive strength results refer to mean compressive strength measured.
214 After testing, the samples were examined for bad compaction and visual porosity. It can be
215 observed all GnS enhanced samples were well compacted with visual pores similar to those of
216 the reference paste (Figure 2).

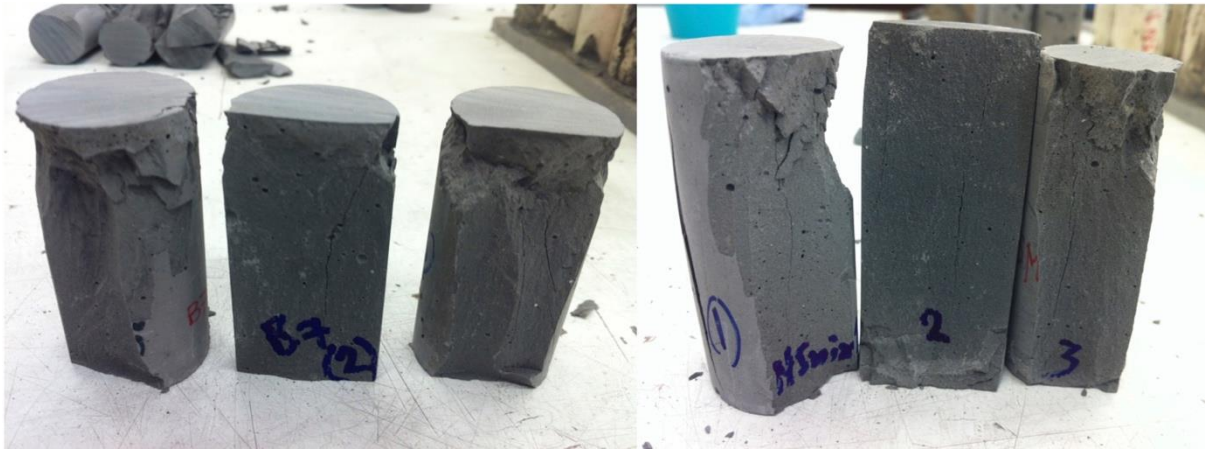

Figure 2: Reference paste (left) and GnS nanomodified cement pastes (right)

Themogravimetric analyses (TGA) - Thermal gravimetric analyses (TGA) were carried out using a Setaram TGA92 instrument. 20 mg of each sample were placed in an alumina crucible and heated at a rate of 10°C/min from 20°C to 1000°C under 100 mL/min flow of inert nitrogen gas. The differential thermal gravimetric (DTG) curve was derived from the TG curve. Buoyancy effects were taken into account, by correcting the curves via automatic blank curve subtraction.

Three different areas as distinguished by the themogravimetric (TG) analyses are of particular interest:

The first one is related to the dehydration of C–S–H, ettringite, gehlenite between 100^{o}C and 180^{o}C and monosulfate between 185^{o}C and 200^{o}C (Collier 2016; Lawrence et al. 2006) and between 270^{o}C and 380^{o}C (Papadakis 1999). It can be postulated that the greater the loss measured the greater the amount of C–S–H and ettringite was produced by the hydration of the paste.

The second area of interest is associated with the dehydration of $Ca(OH)_2$ between 440^{o}C and 510^{o}C:

$$Ca(OH)_2 \rightarrow CaO + H_2O \uparrow$$ Equation: 1

The amount of $Ca(OH)_2$ present in the paste at different ages can be computed by the stoichiometric elaboration of the mass loss results within the specific temperature range:

$$Ca(OH)_2 = \frac{Ca(OH)_2\ related\ H_2O\ mass\ loss \times 74}{18}$$ Equation: 2

Where, 18 = atomic mass of H_2O and 74 = atomic mass of $Ca(OH)_2$.

Therefore, Mass of $Ca(OH)_2$ = (dTG recorded between 440-510^{o}C) / 0.24 Equation: 3

The third area of interest is the decomposition of $CaCO_3$ occurring between 700^{o}C and 810^{o}C according to the following chemical reaction:

$$CaCO_3 \rightarrow CaO + CO_2 \uparrow$$ Equation: 4

The amount of $CaCO_3$ present in the paste at different ages can be computed by the stoichiometric elaboration of the mass loss results within the specific temperature range. If it is greater than the limestone content of the reference paste, it constitutes an indication of sample carbonation.

$$CaCO_3 = \frac{CaCO_3\ related\ CO_2\ mass\ loss \times 100}{44}$$ Equation: 5

Where, 100 = atomic mass unit of $CaCO_3$ and 44 = atomic mass unit of CO_2.

Therefore, Mass of $CaCO_3$ = (dTG recorded between 700-810^{o}C) / 0.44 Equation: 6

Microstructural characterisation - Scanning electron microscopy (SEM) - A set of SEM images was collected for each of the three GnS modified formulations at day 28. A backscattered electron detector was used to capture images of the as received, uncoated, samples.

C. Mathematical elaboration

1. Correlating hydration characteristics with mechanical strength performance in nanomodified cement pastes

The high correlation between the consumption of calcium hydroxide towards he formation of hydration products (microscale characteristics) and the delivered compressive strengths (macroscale performance) of the GnS modified pastes with respect to time has been expressed through a newly introduced ratio. This ratio comprises of the compressive strength of the pastes versus the $Ca(OH)_2$ content, as detected by the TGA/dTG analyses, plotted against time. It was found to give an interesting representation of the performance of composite cement paste formulations. The analyses were carried out on reference paste PC60LS20FA20, accounting for a ratio of PC to FA content of: PC/FA/LS = 3/1/1.

2. Long-term relative density of mortars

BS EN 12390-7:2000, which is designated for hardened concrete with limitations on the maximum coarse aggregate size was selected as a basis for the long-term relative density measurements of the mortars. The volume of the specimen was obtained by water displacement because this method is suitable for specimens of irregular shape. Moreover, although the method is normally unsuitable for "specimens of no-fines concrete, lightweight aggregate concrete with large pores, or specimens whose moisture content must not be altered" since the nanomodified mortars are composed of a wide range of fines it was concluded that indeed this method can also be adapted for the long-term relative density measurements of mortars.

The volume of the specimen, is given by the formula:

$$V = \frac{m_a - m_w}{\rho_w}$$ Equation: 7

Where, m_a = the mass of the specimen in air, in kg, m_w = the apparent mass of the immersed specimen in water, in kg, ρ_w= is the density of water, at 20 °C, taken as 998 kg/m³.

$$D = \frac{m_a}{V}$$ Equation: 8

Where, D is the relative density in kg/m^3.

3. Results & Discussion

3.1 Characterization of nanoparticles of SiO_2

The particle size of GnS in the colloidal solution was investigated by transmission electron microscopy (TEM). TEM analysis showed a significant variation in the bulk of this commercial nS. The diameter of the GnS particles was generally about 5-8 nm (Figure 3-A). However, it is shown by the 10,000 times magnification TEM micrograph that there are some large agglomerations of about 100 nm diameter (Figure 3-B) and also some very small particles of about 2-4 nm diameter (Figure 3-C).

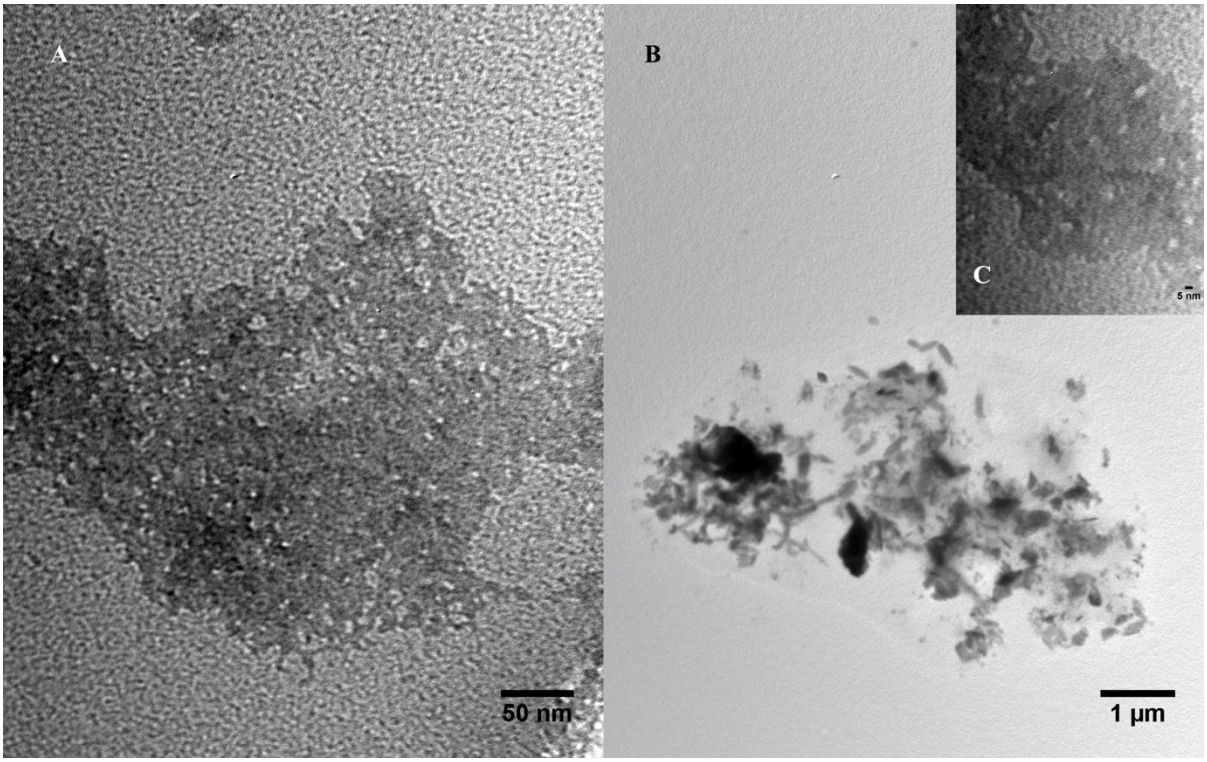

286

287 Figure 3: TEM micrograph of GnS (A) @ 100,000x and (B) @ 10,000x magnification

288

289 Table **2** contains indicatively the first 5 spectra from the 5 x 5 matrix of spectra collected for
290 the elemental analysis (SEM/EDX) from the most homogeneous area depicted in the first
291 micrograph of Figure 3. GnS exhibits traces of SiO_2 and over 70% (normalized atomic) carbon
292 content. It could therefore be more appropriately described as poly-carboxylate dispersion with
293 limited quantities of nS particles. Adding to this, in GnS, the high amount of carbon present is
294 more prone than the nS itself to have significant effects in any GnS nanosilica modified cement
295 pastes. The sulfur present is not likely to affect the hydration as it is commonly used for curing
296 of agents used for the functionalisation of nanosilica (Pourhossaini & Razzaghi-Kashani 2012).

297

298 Table 2: SEM/EDX counts summary (100% atomic) of GnS [5 of 25 spectra]

GnS - All results in atomic % normalized to 100%					
Spectrum	C	O	Na	Si	S
(1,1)	70.58	28.43	0.48	0.12	0.40
(2,1)	70.74	28.38	0.37	0.09	0.42
(3,1)	70.83	28.18	0.40	0.11	0.47
(4,1)	69.19	29.32	0.40	0.21	0.88
(5,1)	72.04	25.15	0.21	0.19	2.41
Mean	71.42	26.66	0.41	0.23	1.28
Std. deviation	1.29	2.04	0.12	0.20	1.37
Max.	74.68	29.32	0.61	0.94	5.41
Min.	68.76	19.35	0.18	0.09	0.39

299

300 Additional TEM imaging of the GnS sample showed a great diversity of agglomerates present;
301 as depicted in Figure 4, Zn rich spheres (Figure 4-A), large Ca-S nanocrystals (Figure 4-B) and
302 other agglomerates of organic matter were also present (Figure 4-C). These limited areas show
303 that this polycarboxylate nS dispersion is not as homogeneous as the aqueous nS dispersions
304 (Calabria-Holley & Papatzani 2014; Papatzani 2016). Consequently, an additional set of
305 spectra was collected from each of these areas, including the large agglomerated nS particles
306 shown in Figure 3-B, in order to investigate the variability in the elements present. The
307 normalized by 100% atomic results are given in Table 3. It is shown that depending on the
308 selected area of sample, certain elements are present, which, however, do not exist in the other
309 areas. Such variability is expected to deliver variabilities of the performance of the nS
310 suspension in composite cementitious binders.

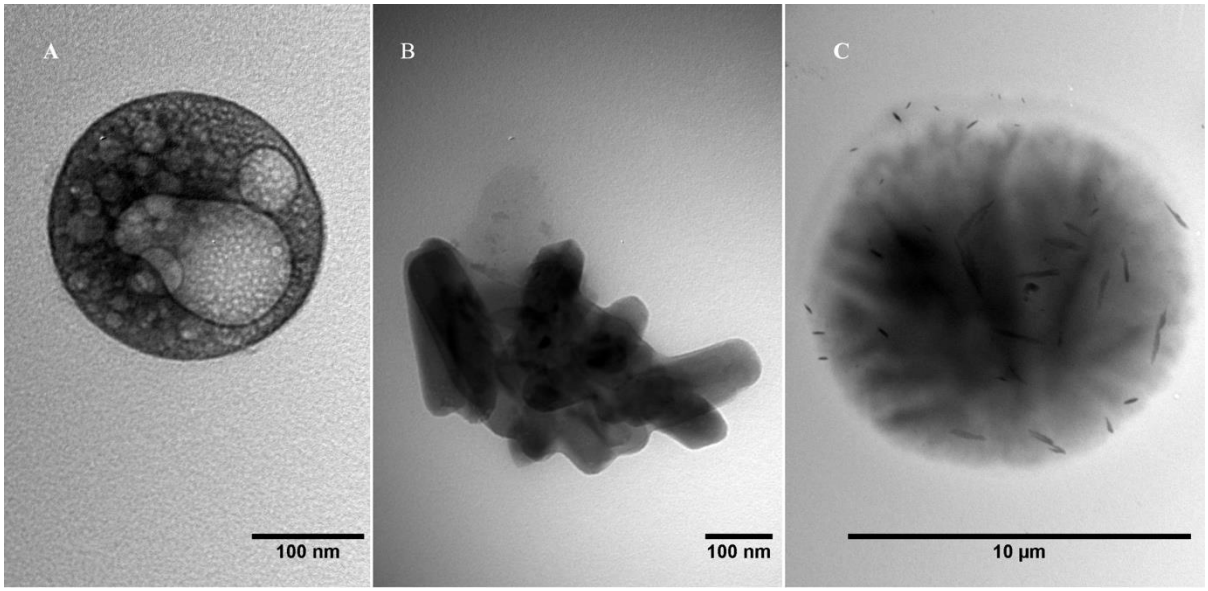

311

312 Figure 4: Chemical elements of GnS determined via TEM

313

314 Table 3: TEM/EDX counts summary (100% atomic) of GnS from Figure 3-B and Figure 4

Spectrum	C	O	Si	S	Ca	Fe	Ni	Cu	Zn
Large agglomerated particles figure 3-B	71,38	10,58	0,71	0,76	0,48	0,91	13,22	1,95	-
Very small nS particles <5nm figure 3-C	73,93	3,96	0,68	-	-	-	9,37	11,32	0,74
Zn rich spheres - figure 4-A	47,15	28,31	-	5,19	-	-	7,48	-	11,87
Large Ca-S rich nanocrystals figure 4-B	57,25	25,65	-	3,31	2,82	-	10,96	-	-

315

316 **3.2 Characterization of quaternary cement formulations with GnS on PC60LS20FA20**

317 Three pastes were produced through the GnS modification of reference paste PC60LS20FA20.
318 The results presented in this section constituted a standalone study on the application of GnS in
319 composite cement pastes and the presence of 60% of PC (clinker) by total mass of binder
320 facilitated the interpretation of the results. Further studies on reduced PC content quaternary
321 cement formulations necessitate the current study in order to better understand the effect of the
322 specific, commercial nS dispersion which also contains polycarboxylates. For this reason, apart
323 from the water to binder (w/b) ratio of 0.3 which is a suitable ratio for nS enhanced pastes
324 (Papatzani, Paine & Calabria-Holley 2014; Papatzani 2016; Calabria-Holley et al. 2015;
325 Papatzani et al. 2015; Папатзани et al. 2014), two lower ones were also investigated; w/b 0.2
326 and 0.22 in an effort to draw the limit between enhancements and limitations. The main results
327 are presented below.

328 **A. Compressive strength of PC/FA/LS=3/1/1 GnS modified pastes**

329 As can be seen in Figure 5 for the same amount of GnS (0.3% by mass) the higher w/b ratio
330 proved to be less favourable. Furthermore, for the lower w/b ratios the higher GnS content
331 exhibited a better performance than the reference paste for the first 28 days. In the effort to set
332 a lower bound in these quaternary pastes the supplier's recommendations were followed to
333 begin with (0.3% of nS solids in these pastes) at 0.3 w/b ratio. This addition did not offer
334 strength enhancement. Then the w/b ratio was reduced to 0.2, still with no improvement.
335 Lastly, the nS particles dosage was increased, while marginally increasing the w/b ratio to 0.22
336 to achieve the desired performance, which can be further improved. The lower compressive
337 strengths of the 0.3% GnS content formulations can be attributed to less homogeneous
338 dispersion of the nS particles in the paste, probably due to the fact that the dosage is too low.
339 Therefore, it was concluded that in quaternary cementitious nanocomposites the

polycarboxylate nS addition should not be lower than 0.6% by total mass of binder for w/b ratio in the order of 0.22. Indeed, the 0.6% GnS enhanced specimen showed a better performance. The fact that the mean compressive strength is marginally below that of the control mix can be attributed to experimental limitations with respect to the homogenous dispersion of low dosages of nanoparticles in such nanomodified composite cement pastes. Adding to this, such discrepancies could also be attributed to the significant variation observed by TEM in the bulk of the nS suspension as already discussed. It should be noted at this point, that during the production of the specimens, the ones with the higher w/b ratio exhibited a prolonged setting. It is possible therefore, although not specified by the producer, that the specific polycarboxylate nS dispersions belonged to the "third generation of superplasticizers" the most important feature of which is the presence of polycarboxylate ether (PCE), with a molecular structure that can be manipulated to affect consistence, retention and the rate of strength development (Scrivener 2009). However, there is not enough evidence to distinguish the exact type of chemical used. Specialized experimental tools should be employed for such investigations, e.g. solid state NMR spectroscopy. Hence, the use of a sonicator or any other advanced technique such as on-demand generation of nanofluidic droplets could have eliminated such discrepancies (mixing limitations), minimizing possible agglomeration of the nS particles and the polycarboxylate in the pastes. Agglomeration is expected to influence rheological properties of pastes, density and induce weak zones in compression. However, hydration can be enhanced (Kong et al. 2013). Some mortar cubes were prepared and tested in compression as shown in the last section of the results, confirming this hypothesis of bad dispersion of low GnS contents in cement pastes.

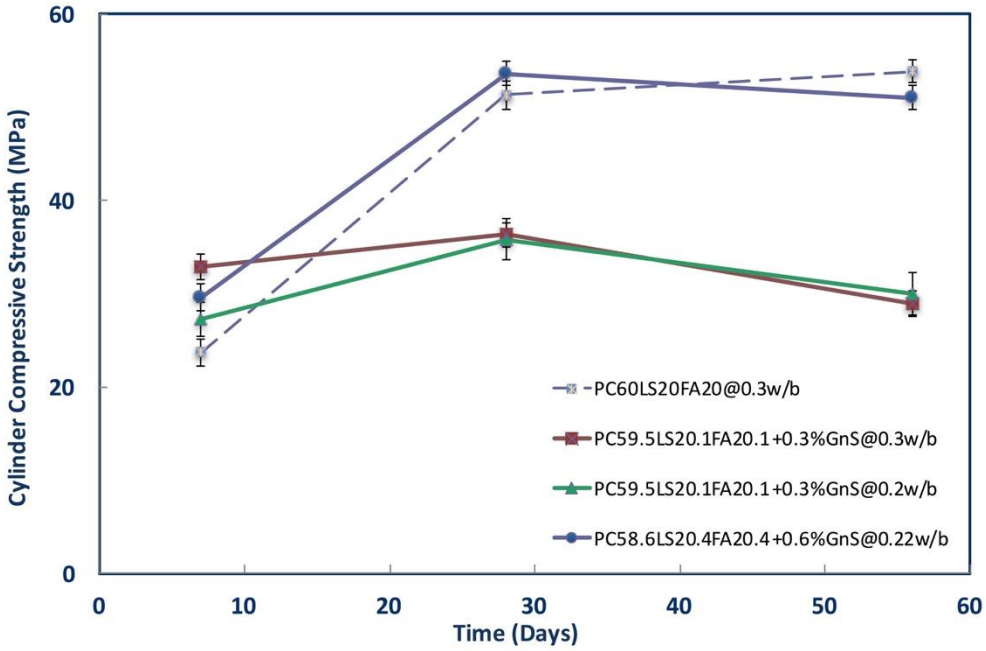

Figure 5: Cylinder compressive strength of GnS modified composite binders

B. Thermal gravimetric analyses of PC/FA/LS=3/1/1 GnS modified pastes

As can be observed in Figure 6-A the $Ca(OH)_2$ content of the reference paste did not change significantly with time. However, the formulation directly comparable to the control paste, i.e. PC59.5LS20.1FA20.1+0.3% GnS @0.3w/b, exhibited significant consumption of $Ca(OH)_2$ only at later ages, as expected due to the water reducing effect of the polycarboxylate and due to the delayed reaction of high FA content pastes with nS (Supit & Shaikh 2015; Papatzani 2016). In fact, the delayed reaction of FA with $Ca(OH)_2$ to form additional C–S–H, lies behind the change in $Ca(OH)_2$ content for all GnS enhanced pastes between 28 and 56 day. Furthermore, the C–S–H formation of PC59.5LS20.1FA20.1+0.3% GnS @0.3w/b at day 7 is similar to that of the control paste (Figure 7-A) and that of day 28 is delayed due to the surface masking of the nS particles by the polycarboxylate and the presence of high FA content (Figure 7-B). Indeed, from day 28 onwards that the reaction of FA is initiated, the amount of C–S–H

formed in paste PC59.5LS20.1FA20.1+0.3% GnS @0.3w/b is significantly greater than that of the control. This finding is in agreement with studies of low PC-high FA quaternary cement pastes enhanced with colloidal aqueous nS particles (PC content 43% and FA content 37% by total mass of binder), in which the pozzolanic activity of FA was pronounced from day 28 until day 56 (Papatzani, Paine & Calabria-Holley 2014). In addition to this, FTIR investigation of quaternary low PC high FA content pastes (PC content 43% and FA content 37% by total mass of binder) at day 28 showed that the GnS enhancement produced pastes with a lower Ca/Si ratio than that of the reference paste, attributed to incomplete C–S–H formation, characteristic of a more polymerized network, which again indicated delay in PC hydration and setting at w/b=0.3, in low PC pastes (Calabria-Holley et al. 2015). It should also be noted that the mass loss observed up to ~75 °C is attributed to residual organic solvent.

Moreover, the two pastes with low w/b ratio exhibited the greatest $Ca(OH)_2$ reduction covering the fact that the hydration products are reduced due to the limited presence of water in the mix. TGA/dTG results presented in Figure 7 indicate that the amount of C–S–H formed in the directly comparable GnS enhanced paste, i.e. PC59.5LS20.1FA20.1+0.3% GnS @0.3w/b, was greater than that in the control paste. Hence, it is clear that GnS exhibited a pozzolanic behaviour, reacting with and consuming $Ca(OH)_2$ at early ages, to produce C–S–H in these pastes. This conclusion is in accordance with the compressive strength results at 7 days which are higher for all GnS enhanced pastes compared with the control. From day 7 to 28, there is enough $Ca(OH)_2$ available for reactions, but the lower GnS content pastes possibly did not have enough available particles to react with and this could be the reason for the marginal increases in compressive strengths from day 7 to 28. Judging by the $Ca(OH)_2$ consumption, from day 28 to 56, significant amounts of C–S–H and other hydration products were formed Figure 7-C, signaling potential increase in compressive strength. The fact that this trend was not observed

for the 56 day strengths was attributed to bad dispersion of the GnS particles in cement pastes overall.

Given that significant changes start at 28 days of curing, the 28-day SEM image analysis was selected for all pastes and is in full agreement with the TGA results as shown in later sections.

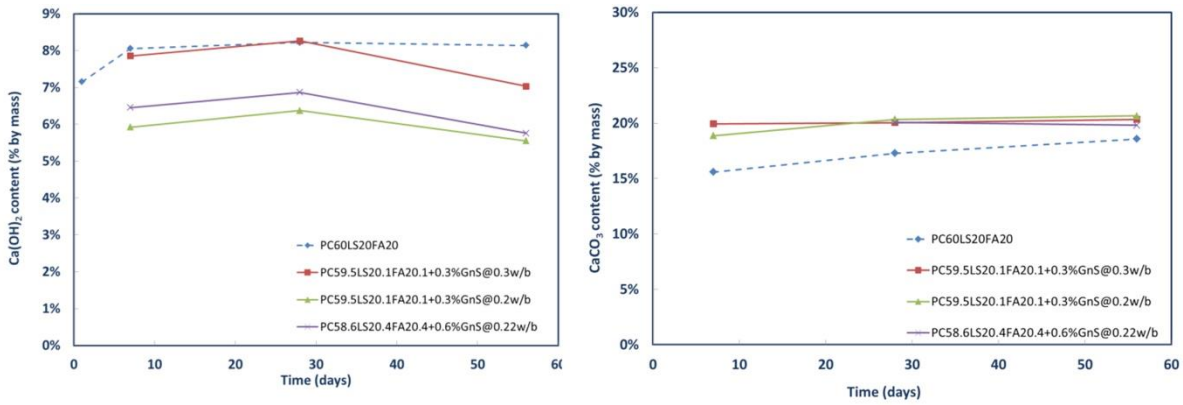

Figure 6: (A) $Ca(OH)_2$ and (B) $CaCO_3$ content of GnS modified composite binders

Another interesting aspect to note is that limestone seems to have interacted with the hydration products formed, inhibiting the decomposition of ettringite to nomosulphate, since no mass loss is observed between 270^{o}C and 380^{o}C (Papadakis 1999) in Figures 7 to 8, in agreement with other researhers suggesting that limestone does not purely act as a filler but also participates in chemical reactions (De Weerdt, Haha, et al. 2011). However, no mass loss was recorded beyond 800^{o}C where, typically, carboaluminates decompose (Esteves 2011).

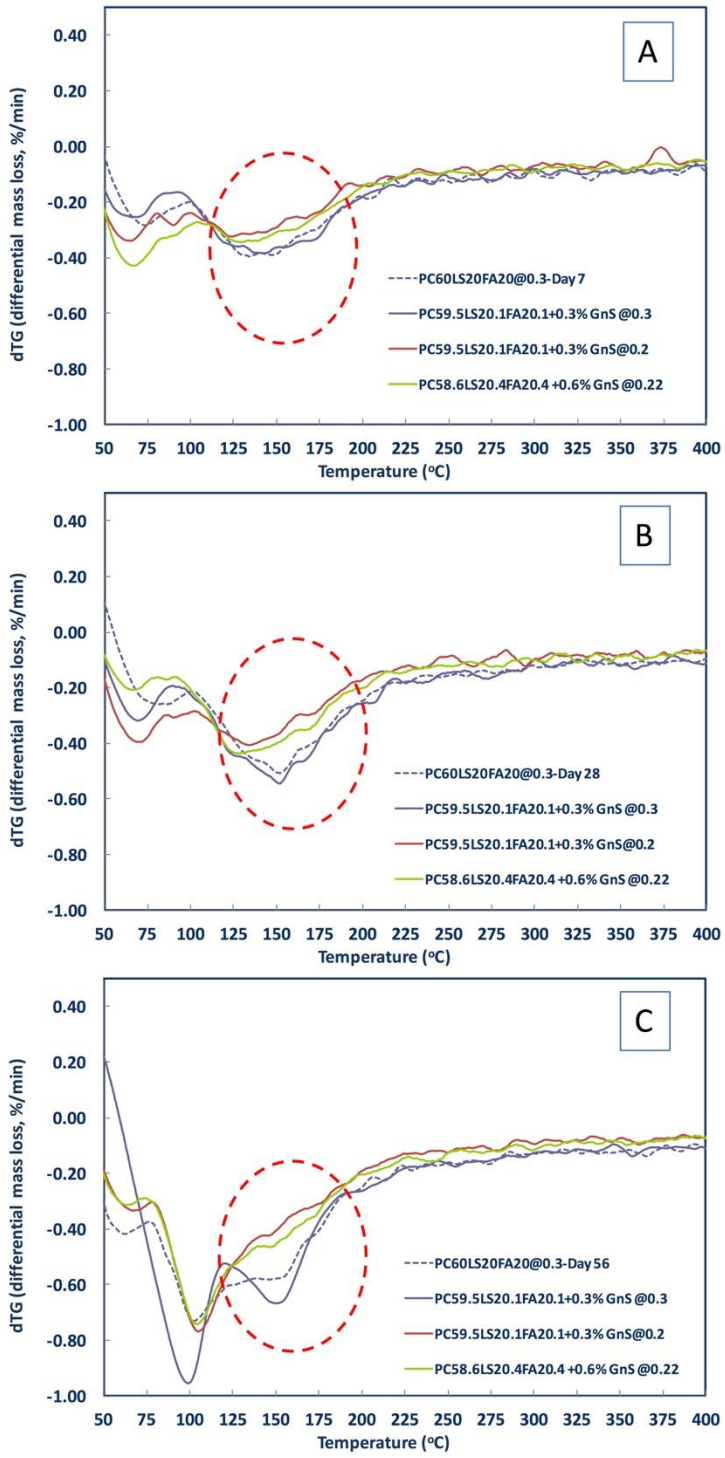

413

414 Figure 7: C–S–H, ettringite and other hydrates, area between 110°C and 170°C (A) at day 7,

415 (B) at day 28 and (D) at day 56 – hydration arrest by oven drying

416

Lastly, the $CaCO_3$ content was significantly increased in the GnS modified pastes (Figure 6-B). However, this observation can be attributed to the high quantities of carbon in the GnS dispersion found with the SEM/EDS elemental analysis, as well as the increased LS content in the mix design.

C. Correlating hydration characteristics with mechanical strength performance in nanosilica modified cement pastes

The ratio of compressive strength of the pastes versus the $Ca(OH)_2$ content is applicable in the quaternary GnS modified pastes. The higher the ratio, the more the related paste outperformed the reference paste. In Figure 8, the superior performance of the lowest w/b ratio paste; PC58.6LS20.4FA20.4+0.6%GnS@0.22w/b is depicted, combining both the higher compressive strength achieved and the more pronounced $Ca(OH)_2$ content consumption. In fact, the paste enhanced with GnS at the same w/b as the control, PC59.5LS20.1FA20.1+0.3%GnS@0.3w/b, which did not seem to have consumed any significant quantities of $Ca(OH)_2$ until day 56, also exhibited the lowest compressive strength. It is also interesting to note that the rate of $Ca(OH)_2$ consumption increased drastically after day 28, presumably because the hydration of PC produced additional quantities of $Ca(OH)_2$ available for reactions. The gradient of the line representing the rate of strength gain of paste PC59.5LS20.1FA20.1 +0.3%GnS @ 0.3w/b was greater, as expected since more water was available for the hydration of cement, which apparently advanced after day 28 in all three GnS modified pastes. It should be noted that the ratio is particularly sensitive to the homogeneity of the pastes and therefore to micropores and other inconsistences. The ratio is proposed herein as an additional mix design criterion for composite cement mix design.

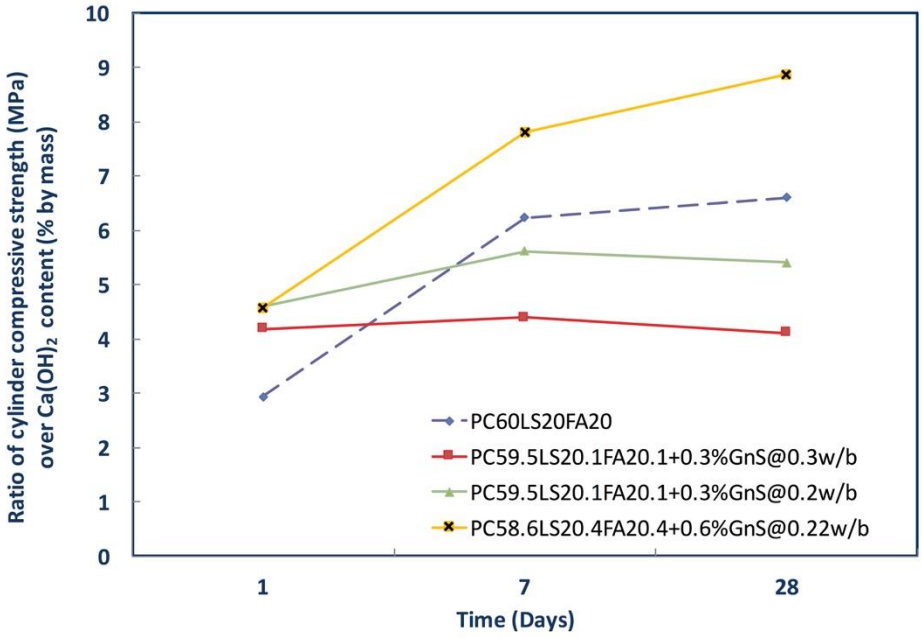

Figure 8: Relating microscale characteristics to macroscale performance of GnS modified composite binders

D. Microstructural characterisation of cement pastes

The microstructural investigations confirmed the findings of compressive strength testing and thermal gravimetric analyses at day 28. In all cases, denser patches of what seems to be C–S–H were identified and marked (CSH for brevity and clarity), indicatively. $Ca(OH)_2$ crystals were covered with C–S–H some of them being individually visible. Although at a first glance the micrographs bear strong similarities, a number of differences can be identified at more careful observation (Figure 9 and Figure 10):

- The number of microcracks reduced drastically with the addition of higher GnS content for w/b = 0.3. However, amongst similar amounts of GnS (pastes PC59.5LS20.1FA20.1+0.3%GnS@0.3 and PC59.5LS20.1FA20.1+0.3%GnS@0.2) the lower w/b ratio mix did exhibit limited microcracks.

- Innumerable reacted FA (rFA) particles, with darker rims surrounding them and a wrapping of hydration products around them were distinguished. The number of unreacted FA particles (uFA) seamed to increase marginally with the reduction of w/b ratio. Paste PC58.6LS20.4FA20.4 +0.6%GnS @0.22, in particular exhibited clusters of unreacted FA particles surrounding rFA.
- The higher the content of GnS the more extended the development of denser patches of what seemed to be C–S–H. A surplus of fibrilar and flake-like formations were identified and assigned to C–S–H, whereas plenty needle-like hydrates, associated with ettringite were also distinguished. The presence of an extended network of flake-like C–S–H is typical of porosity refined pastes (Scrivener & Nonat 2011). Also, a pore is identified with a growth in it (Figure 9-B). For more analytical identifications SEM/EDX should be used.
- Paste PC59.5LS20.1FA20.1+0.3%GnS@0.2 bears great resemblance to paste PC58.6LS20.4FA20.4+0.6%GnS@0.22. The latter, which also showed the best mechanical performance, exhibited the densest microstructure with few microcracks (Figure 10). Furthermore, the magnification of Figure 10-C revealed dense hydration products bridging (area indicated by the arrow) hydrated cement grains, representative of the seeding effect of the GnS nanoparticles. Moreover, the magnification of Figure 10-C also revealed another area (shown in a circle) around a reacted fly ash particle surrounded by unreacted particles of FA, which, in turn, lie in the middle of what seems to be dense C–S–H area. It is possible that the C–S–H gel produced by the pozzolanic reaction of GnS, has been formed around these unreacted FA particles, acting as ion penetration barrier, hence, inhibiting the homogeneous cement hydration (Hou et al. 2012). Such phenomenon may also be observed in hydrating concrete formulations, but a separate study investigations should clarify such hypothesis. Furthermore, the

480 diameter of the FA particles used varied from 1 to 12 μm, with a mean diameter of 9.09
481 μm, as determined by particle size distribution analysis described elsewhere (Papatzani
482 2014). The size of the FA particles does not seem to have affected their reaction
483 potentials in these pastes.

484

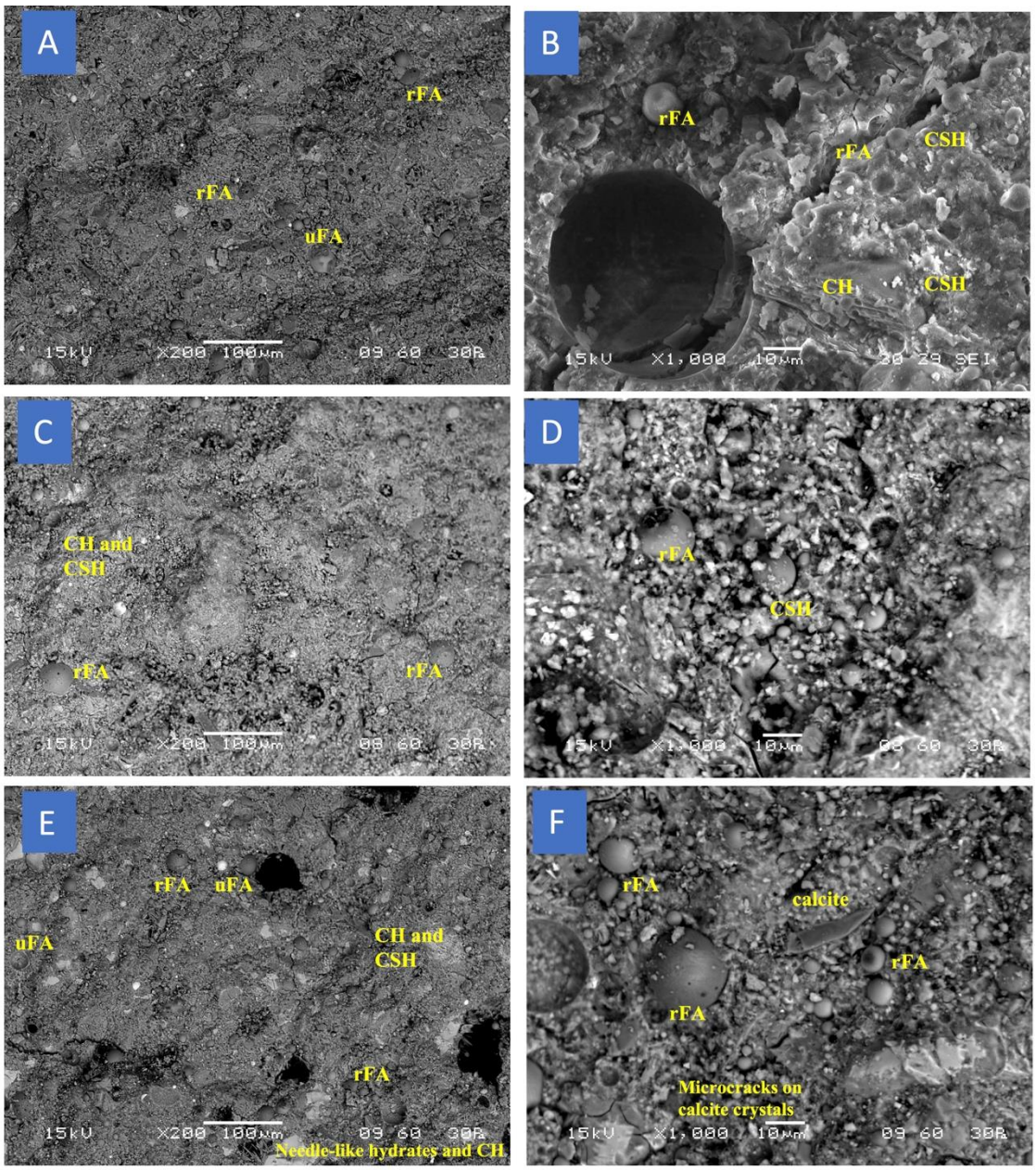

485

486 Figure 9: SEM back scattered micrograph of (A) PC60LS20FA20@0.3-28D - at 200x and
487 (B) at 1000x magnification. (C) PC59.5LS20.1FA20.1+0.3%GnS@0.3-28D - at 200x and
488 (D) at 1000x magnification. (E) PC59.5LS20.1FA20.1+0.3%GnS@0.2-28D -28D at 200x
489 and (F) at 1000x magnification

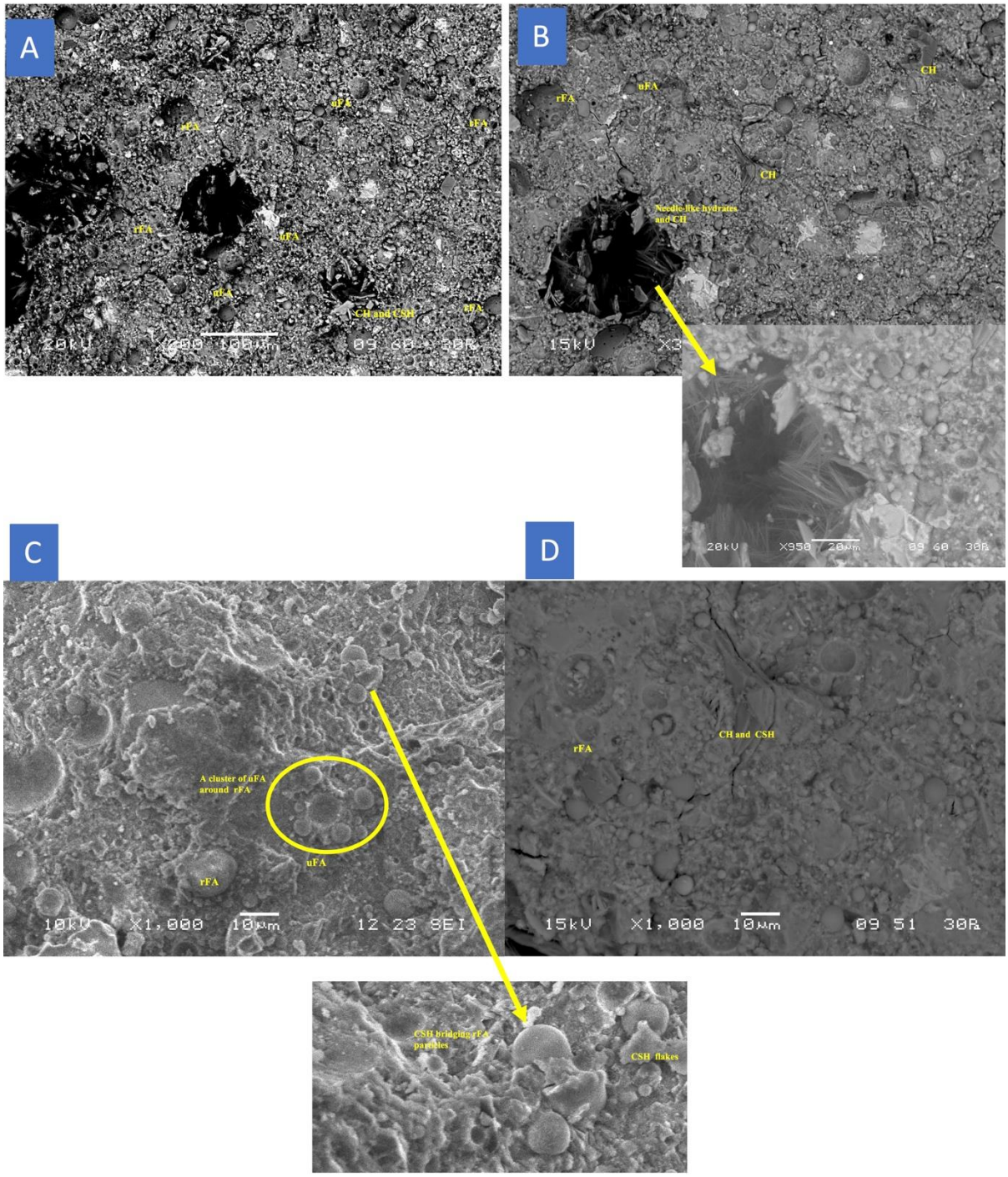

490

491 Figure 10: SEM back scattered micrograph of PC58.6LS20.4FA20.4+0.6%GnS @0.22-

492 28D; (A) 28D –200x, (B) 28D –350x with a detail at 950x, (C & D) 28D –1000x, with a

493 detail at 3000x magnification

494

E. Compressive strength tests and late age relative density of mortars

To confirm the understanding on the behaviour of GnS modified pastes, the simplest combination based on PC100 (denoted as M.PC100) using CEMI-45R for simplicity (rather than CEM II/A-L 42,5 which was used for all pastes) with a w/b ratio of 0.5 was selected. Then, it was nanomodified by adding 0.25% or 0.50% GnS by mass of CEMI at a reduced w/b ratio and tested in compression at day 7, 28, 56 and 90. The higher dosage of GnS, i.e. that of 0.5% by mass of binder, at lower w/b ratio offered significant improvements, maintaining and increasing strengths with time (Figure 11-A). In full accordance with the compressive strength of pastes, the most pronounced improvement in strength is achieved at early ages; day 7 and day 28. The lower GnS content showed the greatest strength diversity, with a sharp reduction of strength at day 90 attributed to non-homogeneous dispersion of the few GnS particles in the mass of the mortars. Therefore, the lower bound of GnS addition is reached and is equal to 0.5% by total mass of binder.

Knowing that the theoretical maximum density of PC is 3250 kg/m^3, that of sand is 2650 kg/m^3 and of water 1000 kg/m^3 the theoretical maximum density for a mortar of 100% PC at w/b = 0.5 was found to be equal to 2600 kg/m^3. Therefore, judging by the late age (after month 6) relative density measured (Figure 11-B) the M.PC100 did not seem to contain significant pores. The addition of GnS (M.PC99.5+0.5%GnS) offered higher densities, probably due to the particle packing effect. However, the higher dosage of GnS marginally reduced density, although the strength increased. This could be explained by the fact that the addition of greater amounts can cause agglomeration of the particles within the hydrating paste and consequently, increase the porosity hence reduce relative density, although the chemical effect of increased hydrations reactions towards the production of additional C–S–H is accomplished offering higher compressive strengths. It should be noted that the theoretical maximum density of the nanomodified mortars could not be calculated due to lack of data on the theoretical density of the nanoparticles.

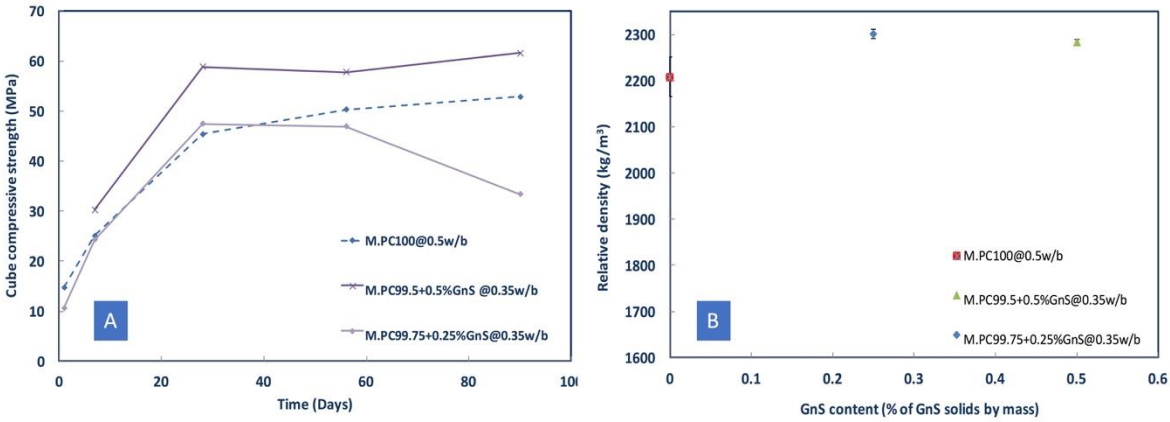

520

521 Figure 11: (A) Cube compressive strength of GnS modified mortars based on PC100 &

522 (B) Relative density of GnS modified mortars based on PC100

523

524 **4. Conclusions**

525 This study is the first presented involving composite binders of lower than the Eurocode
526 designated clinker content and nanosilica particles dispersed in organic (polycarboxylate)
527 medium. The complex chemistry involved in the dispersion has affected the hydration, the
528 microstructure and the strength development of the composite binders produced. From the
529 above, it can be postulated that GnS, if added at reduced w/b ratio, can enhance hydration
530 reactions and the microstructure. Which, in turn is expected to lead to long term durability and
531 mechanical performance superior than that of the reference paste, for PC/FA/LS ratio of 3/1/1.
532 The lower bound of GnS addition was determined to be 0.6% by mass of binder for cement
533 pastes, whereas for mortars it can reach 0.5% by mass of binder. Moreover, it is possible that
534 greater quantities of GnS can be added in blended cements of PC/FA/LS =3/1/1, as the thermal
535 gravimetric analyses showed that there was $Ca(OH)_2$ available for pozzolanic reactions.
536 However, if the increase in GnS content is at the expense of PC content, care should be taken
537 so that the hydration of Portland cement can advance, notwithstanding the reduction of w/b

538 ratio, which is necessary for the greater GnS additions. This limitation is more pronounced with
539 polycarboxylate / nS dispersions, such as GnS compared to their aqueous counterparts. As was
540 observed in Figure 5 for the same w/b ratio (0.3) the addition of even minor (0.3% by mass)
541 polycarboxylate nS dispersions can be unfavourable, probably due to delayed setting and
542 obstruction of the hydration reactions. However, a small reduction in the w/b ratio (0.22)
543 accompanied by an increase in the GnS content (0.6% by mass) proved to be more successful
544 in these pastes than a more drastic reduction in w/b ratio (0.2) and low amount of GnS (0.3%
545 by mass). Other mediums such as sulphonated naphthalene formaldehyde could be a used for
546 the dispersion of the nS particles, avoiding extensive quantities of carbon found in the
547 dispersion under investigation. However, for the purpose of this study a commercially available
548 product was used as received and its suitability for composite binders of lower clinker content
549 than the recommended by the Eurocodes was scrutinized. It should be noted though, that
550 extensive research carried out by the authors indicates that improvements in hydration,
551 microstructure and mechanical strengths are secured with the use of aqueous dispersions,
552 allowing the clinker to be reduced to 43%, probably due to less complicated chemistry involved
553 (Papatzani, Paine & Calabria-Holley 2014; Papatzani 2015; Calabria-Holley & Papatzani 2014;
554 Papatzani, Paine, Calabria-Holley, et al. 2014).

555 On the other hand, GnS dosage should be limited as the C–S–H gel produced may be acting as
556 ion penetration barrier around FA particles, blocking composite cement paste homogeneous
557 hydration, a matter that can arise in concrete design, as well. Most importantly, given that the
558 depletion of $Ca(OH)_2$ is not an issue, since significant quantities were detected with TG as well
559 as with SEM, the other hypothesis could be that GnS addition abruptly dropped the pH of the
560 hydrating composite cement paste, which, in turn, did not allow the vitreous phase of FA to
561 decompose and consequently engage in pozzolanic reactions. Therefore, although there is
562 $Ca(OH)_2$ and FA available in the paste, these “FA particles of non-decomposed vitreous phase”

cannot react with $Ca(OH)_2$ and produce additional C–S–H beyond day 28. This hypothesis can also explain the reduction in the mean compressive strength of the GnS enhanced pastes at day 56. For this, it can be said that, in the GnS modified composite cements with PC/FA/LS=3/1/1 (PC60LS20FA20), the constituents of the binder seem to bear antagonistic features between their functionalities. Further studies should clarify safe upper bounds of GnS addition and also potential hydration blocking mechanisms in concrete formulations utilizing these nanocomposite binders. In addition to the interaction of FA with GnS, the w/b ratio must be regulated with respect to the GnS content and the homogeneous dispersion of the nS particles in the binder must be secured, as discussed.

Nanotechnologists are expected to contribute towards the development of new methods that will allow homogeneous dispersion of nanoparticles in the bulk of composite cements matrices for industrial applications and for mass production of nanomodified concrete. Studies like the one presented in this paper are necessary in order to shed light to the effect of nanoparticles in quaternary cement formulations especially since data-sheets of commercial nanoparticles contain information related to mortars rather than pastes. The presented research also highlights the fact that, in the case of GnS added composite binders, supplier's recommendations do not suffice. Binder testing should precede concrete design. Such studies pave the way for further investigation of more challenging nanocements, such as those of very low PC and high FA content, leading to innovative green cements unattainable, in the past, without the help of nanotechnology.

5. Acknowledgements

Authors acknowledge the European Commission funding (FIBCEM project, grant Number 262954) and all partners are thanked for their input and for the supply of materials.

The authors would also like to thank the Department of Chemical Engineering at the University of Bath for the use of the TG analyser.

6. References

Björnström, J. et al., 2004. Accelerating effects of colloidal nano-silica for beneficial calcium–silicate–hydrate formation in cement. *Chemical Physics Letters*, 392(1–3), pp.242–248. Available at: http://www.sciencedirect.com/science/article/pii/S0009261404007730.

BS, E.N.-, 2005. Methods of testing cement. *Part 1: Determination of strength*, BS EN 196-(1), p.36.

Bye, G., Livesey, P. & Struble, L., 2011. *Portland Cement* P. Livesey & L. Struble, eds., ICE Publishing. Available at: http://www.icevirtuallibrary.com/doi/abs/10.1680/pc.36116.

Calabria-Holley, J., Paine, K. & Papatzani, S., 2015. Effects of nanosilica on the calcium silicate hydrates in Portland cement–fly ash systems. *Advances in Cement Research*, 27(4), pp.187–200. Available at: http://dx.doi.org/10.1680/adcr.13.00098.

Calabria-Holley, J. & Papatzani, S., 2014. Effects of nanosilica on the calcium silicate hydrates in Portland cement-fly ash systems. *Advances in Cement Research*, 26(1), pp.1–14.

CEN, 2000. Cement - Part 1: Composition, specifications and conformity criteria for common cements. , EN 197-1:2(1), p.29.

609 Collier, N.C., 2016. Transition and decomposition temperatures of cement phases - a
610 collection of thermal analysis data. *Ceramics - Silikaty*, 60(4), pp.338–343.
611 Esteves, L.P., 2011. On the hydration of water-entrained cement–silica systems: Combined
612 SEM, XRD and thermal analysis in cement pastes. *Thermochimica Acta*, 518(1–2),
613 pp.27–35.
614 Hou, P. et al., 2012. Effects of colloidal nanoSiO2 on fly ash hydration. *Cement and*
615 *Concrete Composites*, 34(10), pp.1095–1103. Available at:
616 http://www.sciencedirect.com/science/article/pii/S0958946512001400.
617 Kong, D. et al., 2013. Influence of nano-silica agglomeration on fresh properties of cement
618 pastes. *Construction and Building Materials*, 43(0), pp.557–562. Available at:
619 http://www.sciencedirect.com/science/article/pii/S0950061813001955.
620 Lawrence, R.M.H. et al., 2006. The use of TG to measure different concentrations of lime in
621 non-hydraulic lime mortars. *Journal of Thermal Analysis and Calorimetry*, 85(2),
622 pp.377–382.
623 Meyer, C., 2009. The greening of the concrete industry. *Cement and Concrete Composites*,
624 31(8), pp.601–605. Available at:
625 http://www.sciencedirect.com/science/article/pii/S0958946509000031.
626 Papadakis, V.G., 1999. Effect of fly ash on Portland cement systems: Part I. Low-calcium fly
627 ash. *Cement and Concrete Research*, 29(11), pp.1727–1736. Available at:
628 http://www.sciencedirect.com/science/article/pii/S0008884699001532.
629 Papatzani, S., 2016. Effect of nanosilica and montmorillonite nanoclay particles on cement
630 hydration and microstructure. *Materials Science and Technology*, 32(2), pp.138–153.
631 Available at: http://www.tandfonline.com/doi/abs/10.1179/1743284715Y.0000000067.
632 Papatzani, S., 2015. Effect of nanosilica and montmorillonite nanoclay particles on cement
633 hydration and microstructure. *Materials Science and Technology; in press*.

634 Papatzani, S., 2014. *Nanotechnologically modified cements: Effects on hydration,*
635 *microstructure and physical properties*. UK: University of Bath.
636 Papatzani, S., Paine, K., Calabria-Holley, J., et al., 2014. Прочность и микроструктура
637 цементного камня с добавками коллоидного SiO2 (Strength and microstructure of
638 colloidal nanosilica enhanced cement pastes (In Russian)). *Цемент и его применение*
639 *(Cement and its Applications)*, 4, pp.80–85.
640 Papatzani, S., Paine, K. & Calabria-Holley, J., 2015. A comprehensive review of the models
641 on the nanostructure of calcium silicate hydrates. *Construction and Building Materials*,
642 74, pp.219–234. Available at:
643 http://www.sciencedirect.com/science/article/pii/S0950061814011738.
644 Papatzani, S., Paine, K. & Calabria-Holley, J., 2014. The effect of the addition of
645 nanoparticles of silica on the strength and microstructure of blended Portland cement
646 pastes. *May 12-15, International Concrete Sustainability Conference*. Available at:
647 http://www.nrmcaevents.org/?nav=display&file=648.
648 Pourhossaini, M.R. & Razzaghi-Kashani, M., 2012. Grafting hydroxy-terminated
649 polybutadiene onto nanosilica surface for styrene butadiene rubber compounds. *Journal*
650 *of Applied Polymer Science*, 124(6), pp.4721–4728. Available at:
651 http://dx.doi.org/10.1002/app.35514.
652 Raki, L. et al., 2010. Cement and Concrete Nanoscience and Nanotechnology. *Materials*,
653 3(2), pp.918–942. Available at: http://www.mdpi.com/1996-1944/3/2/918.
654 Scrivener, K.L., 2009. Nanotechnology and cementitious materials. *Nanotechnology in*
655 *Construction 3*, pp.37–42.
656 Scrivener, K.L. & Nonat, A., 2011. Hydration of cementitious materials, present and future.
657 *Cement and Concrete Research*, 41(7), pp.651–665. Available at:
658 http://www.sciencedirect.com/science/article/pii/S0008884611001025.

659 Shu, X. et al., 2016. Tailoring the solution conformation of polycarboxylate superplasticizer
660 toward the improvement of dispersing performance in cement paste. *Construction and*
661 *Building Materials*, 116, pp.289–298. Available at:
662 http://www.sciencedirect.com/science/article/pii/S0950061816306833.
663 Singh, L.P.P. et al., 2013. Beneficial role of nanosilica in cement based materials – A review.
664 *Construction and Building Materials*, 47(0), pp.1069–1077. Available at:
665 http://www.sciencedirect.com/science/article/pii/S0950061813004509 [Accessed
666 September 24, 2016].
667 Supit, S.W.M. & Shaikh, F.U.A., 2015. Durability properties of high volume fly ash concrete
668 containing nano-silica. *Materials and Structures*, 48(8), pp.2431–2445. Available at:
669 http://dx.doi.org/10.1617/s11527-014-0329-0.
670 De Weerdt, K., Haha, M. Ben, et al., 2011. Hydration mechanisms of ternary Portland
671 cements containing limestone powder and fly ash. *Cement and Concrete Research*,
672 41(3), pp.279–291. Available at:
673 http://www.sciencedirect.com/science/article/pii/S0008884610002577.
674 De Weerdt, K., Kjellsen, K.O., et al., 2011. Synergy between fly ash and limestone powder in
675 ternary cements. *Cement and Concrete Composites*, 33(1), pp.30–38. Available at:
676 http://www.sciencedirect.com/science/article/pii/S0958946510001368.
677 Zhang, J. & Scherer, G.W., 2011. Comparison of methods for arresting hydration of cement.
678 *Cement and Concrete Research*, 41(10), pp.1024–1036.
679 Папатзани, С., Пэйн, К. & Калабрия-Холли, Д., 2014. Прочность и микроструктура
680 цементного камня с добавками коллоидного SiO2 (Strength and microstructure of
681 colloidal nanosilica enhanced cement pastes (In Russian)). *Цемент и его применение*
682 *(Cement and its Applications)*, 4, pp.80–85. Available at:
683 http://www.cemcom.ru/2014_4%0D.

684

685